How to cite: *Angew. Chem. Int. Ed.* **2021**, *60*, 20558–20562
International Edition: doi.org/10.1002/anie.202108269
German Edition: doi.org/10.1002/ange.202108269

Supramolecular Switch

Cooperative Effects in Switchable Catalysis: Enhancing Double-Click Reaction Yield of Symmetrical Rotaxanes

*Amit Ghosh, Indrajit Paul, and Michael Schmittel**

In memory of Professor Siegfried Hünig

Abstract: *Reversible switching between the closed cyclic dimeric assembly $[Cu_2(\mathbf{1})_2]^{2+}$ (OFF state) and the extended dimeric homoleptic complex $[FeCu_2(\mathbf{1})_2]^{4+}$ (ON State) by addition/removal of Fe^{2+} triggered catalysis of a double-click reaction and high yield preparation of [2]rotaxanes. Mechanistic and computational studies provide valuable general insight for double-click strategies by revealing cooperative effects in the second cycloaddition step due to a distance-tolerant preorganization of the first-click product by the two copper(I)-loaded phenanthroline subunits of $[FeCu_2(\mathbf{1})_2]^{4+}$.*

Introduction

Inspired by Nature, chemists have increasingly developed switchable catalysts that are of great use for ON/OFF or UP/DOWN regulation[1,2] and thus of great promise for autonomous networked reaction systems.[3] Various protocols have been used for the activation of switchable catalysts, for instance the exposure/hiding of the active site(s) in rotaxanes,[4] the unlocking/self-locking[5] of switchable frameworks, and the weak-link approach.[6] The two latter modi operandi allow exposure of not only one but also two active sites in the switching process thus opening venues for distance control in catalysis.[7] Herein, we demonstrate a switchable catalyst system with ON/OFF exposure of two distant catalytic sites[8] that produces far superior amounts of [2]rotaxanes in a double-click[9] reaction than a single-site reference system. The chelate cooperativity[10] exploited here furnishes valuable hints for the general optimization of double-click strategies.

For the preparation of interlocked molecules, which play an eminent role in molecular electronic devices[11] and artificial molecular machines,[12] three distinct template-mediated approaches are of paramount importance. Here, we capitalize on the popular capping (= threading-followed-by-stoppering) strategy using the versatile CuAAC "click" reaction[13] in combination with switchable catalysis to prepare [2]rotaxanes (Scheme 1). To the best of our knowledge, the catalytic preparation of rotaxanes employing an artificial ON/OFF supramolecular catalyst is unprecedented. It could be considered remotely reminiscent of a reaction, though, that was catalyzed by a macrocyclic copper complex.[14]

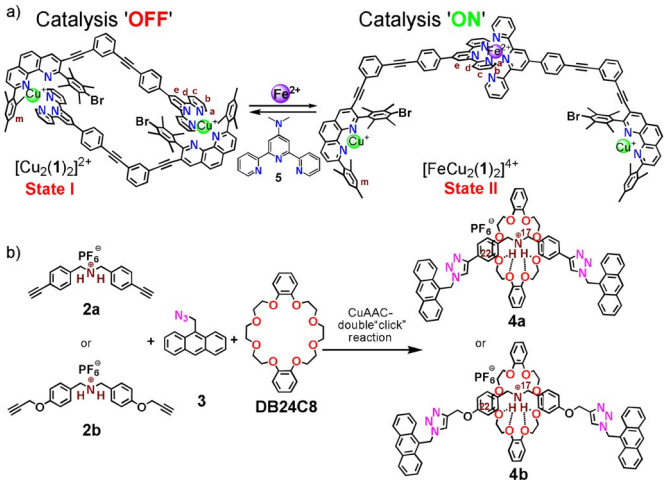

Scheme 1. a) Switching between closed and open form of two dimeric copper(I) complexes. b) General reaction scheme for the synthesis of [2]rotaxanes **4a** and **4b**.

Inspired by a recently reported monomer–dimer nanoswitch,[5b] we designed the closed and open supramolecular complexes $[Cu_2(\mathbf{1})_2]^{2+}$ (State I) and $[FeCu_2(\mathbf{1})_2]^{4+}$ (State II, Scheme 1a), expecting that a reversible close-to-open switching should be feasible due to the distinct coordination properties of copper(I) and iron(II) ions. Moreover, we anticipated that the two exposed copper sites in the open State II would be catalytically active for a double-click reaction, which would allow us to synthesize rotaxanes (Scheme 1b).

Results and Discussion

The literature-known ligand **1** and dimeric complex $[Cu_2(\mathbf{1})_2]^{2+}$ were synthesized according to the established procedures[15] and characterized by ^{1}H NMR (SI, Figures S1 and S29). When 0.5 equiv of $Fe(BF_4)_2$ were added to the red complex $[Cu_2(\mathbf{1})_2]^{2+}$ (State I), the deep violet complex $[FeCu_2(\mathbf{1})_2)]^{4+}$ formed by using exclusively the terminal

[*] Dr. A. Ghosh, Dr. I. Paul, Prof. Dr. M. Schmittel
Center of Micro and Nanochemistry and Engineering
Organische Chemie I, University of Siegen
Adolf-Reichwein Strasse 2, 57068 Siegen (Germany)
E-mail: schmittel@chemie.uni-siegen.de
Supporting information and the ORCID identification number(s) for the author(s) of this article can be found under: https://doi.org/10.1002/anie.202108269.

terpyridine unit for complexation. $[Cu_2(\mathbf{1})_2]^{2+}$ exhibited a sharp absorption at $\lambda = 328$ nm and a weak broad band at 503 nm (SI, Figure S54). Upon addition of iron(II) ions, the absorption at $\lambda = 328$ nm shifted within 40 s to $\lambda = 345$ nm whereas concurrently a new MLCT band evolved at $\lambda =$ 573 nm (SI, Figure S57). In addition, the ^{1}H NMR spectrum showed the typical shifts of terpyridine protons a-H, d-H, and e-H after iron complex formation (Figure 1). Likewise, the

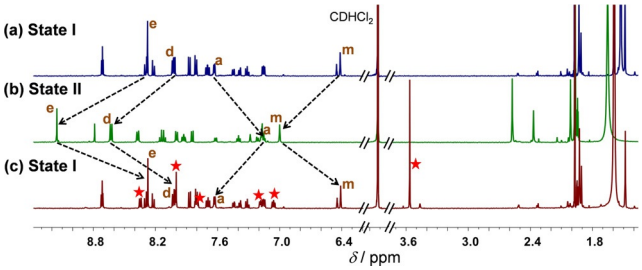

Figure 1. Partial ^{1}H NMR spectra (500 MHz, CD_2Cl_2, 298 K) of **1** after the addition of (a) one equiv of $[Cu(CH_3CN)_4]PF_6$, then (b) 0.5 equiv of $Fe(BF_4)_2$, and finally (c) one equiv of 4-*N*,*N*-dimethylaminoterpyridine (**5**). Red asterisks indicate signals of $[Fe(\mathbf{5})_2]^{2+}$.

downfield shift of the aromatic mesityl proton (m-H) from 6.41 to 7.00 ppm indicated the formation of copper(I)-loaded phenanthrolines. A single trace in the diffusion-ordered spectrum (DOSY) matching a hydrodynamic radius of 11.1 Å suggested the existence of $[FeCu_2(\mathbf{1})_2]^{4+}$ as the only species in solution (SI, Figure S36). The ESI-MS further proved formation of complex $[FeCu_2(\mathbf{1})_2]^{4+}$ by characteristic peaks (SI, Figure S52). Summing up, diagnostic changes in the UV/Vis absorptions, ^{1}H NMR splittings, and ESI mass signals undoubtedly provided support for the formation of the open dimeric complex $[FeCu_2(\mathbf{1})_2)]^{4+}$ that will be denoted as State II in the switching process.

Resetting State I from State II was readily accomplished within 10 s by selective removal of Fe^{2+} (SI, Figure S58). Upon addition of 4′-*N*,*N*-dimethylamino-2,2′:6′,2″-terpyridine (**5**), a strong complexation agent for Fe^{2+}, we observed the immediate and clean formation of $[Cu_2(\mathbf{1})_2]^{2+}$ and $[Fe(\mathbf{5})_2]^{2+}$ by ^{1}H NMR and UV/Vis spectral evidence. Complex $[Cu_2(\mathbf{1})_2]^{2+}$ was safely identified by its mesityl proton signal m-H at 6.41 ppm in the ^{1}H NMR spectrum (Figure 1) and its absorption at $\lambda = 328$ nm (SI, Figure S56). The complete cycle was reproduced six more times (SI, Figure S40).

After establishing reversibility between States I and II via addition and removal of iron(II) ions, the efficiency of the system was evaluated as a switchable transition metal catalyst. In previous work, we had already shown that copper(I)-loaded phenanthrolines of type $[Cu(phenAr_2)]^+$ were able to catalyze cyclopropanations[5b] and click reactions.[2d] Equally, the exposed copper(I) ions in the dimer $[FeCu_2(\mathbf{1})_2)]^{4+}$ (State II) should be capable of capping bis-ethynyl terminated pseudorotaxanes with bulky stoppers via a click[16] protocol to form [2]rotaxanes. No catalytic activity was expected for complex $[Cu_2(\mathbf{1})_2]^{2+}$ since the encapsulated copper(I) ions should be unreactive.

To test this hypothesis, the linear diethynyl ammonium ions **2a** or **2b** were selected due to their propensity to thread into the dibenzo-24-crown-8 macrocycle (**DB24C8**) by non-covalent interactions. The intermediate pseudorotaxane should then be convertable to either rotaxane **4a**[17] or **4b** via a double CuAAC "click"[13] reaction using an excess amount of azide **3** (Scheme 1b). The latter was chosen due to the bulky anthracene moiety preventing dethreading of the **DB24C8**.

In detail (Figure 2), when a 1:5:4 mixture of **2a** (or **2b**), **DB24C8** and **3** was heated at 40 °C in the presence of the closed complex $[Cu_2(\mathbf{1})_2]^{2+}$ (10 mol %) for 42 h (or 120 h for

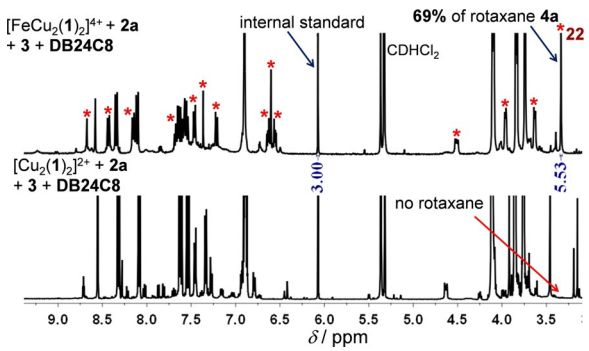

Figure 2. ^{1}H NMR (400 MHz, CD_2Cl_2, 298 K) after reacting **2a**, **3**, and **DB24C8** for 42 h at 40 °C either in the presence of $[Cu_2(\mathbf{1})_2]^{2+}$ or $[FeCu_2(\mathbf{1})_2]^{4+}$. Red asterisks indicate signals of rotaxane **4a**. 1,3,5-Trimethoxybenzene was used as internal standard.

2b), no rotaxane was observed as expected. However, when the experiment was performed under identical conditions in presence of the open complex $[FeCu_2(\mathbf{1})_2)]^{4+}$ (10 mol %), (69 ± 3) % of rotaxane **4a** was afforded (Figure 2). During the reaction some material precipitated that was identified as the axle without macrocycle (SI, Figure S83). Alike, when a 1:5:4 mixture of **2b**, **DB24C8**, and **3** was heated at 40 °C for 120 h in the presence of complex $[FeCu_2(\mathbf{1})_2)]^{4+}$ (10 mol %), the reaction produced (75 ± 3) % of rotaxane **4b** (SI, Figure S87). Rotaxanes **4a** and **4b** were characterized by ^{1}H NMR, ^{13}C NMR and electrospray mass spectroscopy (ESI-MS) (SI, Figures S19–S23, S45, and S46).

Finally, multiple OFF/ON switching of the catalysis was probed in situ toward formation of rotaxane **4a** (Figure 3). As before, the reaction of a 1:5:4 mixture of **2a**, **DB24C8**, and **3** in presence of 10 mol % of $[Cu_2(\mathbf{1})_2]^{2+}$ (State I) did not furnish any of the mechanically interlocked rotaxane **4a** after heating at 40 °C for 15 h (SI, Figure S105a). However, after addition of 0.5 equiv of $Fe(BF_4)_2$ to this mixture, heating at 40 °C for 15 h generated the rotaxane **4a** in (18 ± 3) % yield (SI, Figure S105b). To trap the iron(II) ions and regenerate State I, 4′-*N*,*N*-dimethylamino-2,2′:6′,2″-terpyridine (**5**) and consumed amounts of compounds **2a**, **DB24C8**, and **3** were added. Heating the latter mixture at the same conditions produced no rotaxane (SI, Figure S105c). When the full cycle was repeated a second time with Fe^{2+}, it provided rotaxane **4a** in 34 % overall yield (SI, Figure S105d), thus yielding 16 % product in the second cycle.

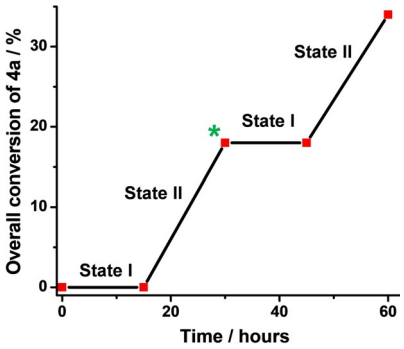

Figure 3. Reversible switching between the closed $[Cu_2(\mathbf{1})_2]^{2+}$ and the open $[FeCu_2(\mathbf{1})_2)]^{4+}$ (10 mol%) in the presence of **2a**, **DB24C8**, and **3** in a 1:5:4 ratio. Heating State II for 15 h at 40 °C furnished reproducible amounts of [2]rotaxane **4a** (two independent runs). Consumed amounts of substrates were added (see green asterisk).

Finally, the question was addressed whether the two spatially separated copper(I) phenanthrolines in $[FeCu_2(\mathbf{1})_2)]^{4+}$ would act in a cooperative manner. Hereunto the efficiency of $[FeCu_2(\mathbf{1})_2)]^{4+}$ was compared with that of the copper(I)-loaded systems $[Cu_2(\mathbf{6})]^{2+}$ and $[Cu(\mathbf{7})]^{+}$ (Scheme 2a, Table 1), both of them equipped with close mimics of the catalytic copper(I) sites in $[FeCu_2(\mathbf{1})_2)]^{4+}$. Both double-copper(I) catalysts $[FeCu_2(\mathbf{1})_2)]^{4+}$ and $[Cu_2(\mathbf{6})]^{2+}$ clearly generated much higher yields of rotaxane **4a** than the mono-copper(I) catalyst $[Cu(\mathbf{7})]^{+}$. To evaluate distance aspects in this double functionalization, the larger dialkyne **2b** (Table 1) was tested as well. Here, $[FeCu_2(\mathbf{1})_2)]^{4+}$ was highly active whereas both the double-copper(I) catalyst

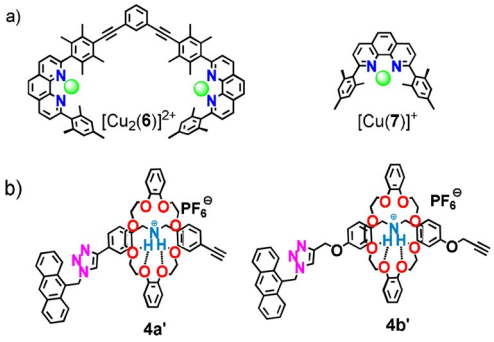

Scheme 2. a) Two CuAAC catalysts as reference systems. b) The intermediate monotriazole pseudorotaxanes.

Table 1: Yields of click products **4a**,**b** using various catalysts.

Catalyst	Yield [%] (±3%)			
	4a[a,c]	**4a**[b]	**4b**[a,d]	**4b**[b]
$[FeCu_2(\mathbf{1})_2)]^{4+}$[e]	69	73	75	82
$[Cu_2(\mathbf{6})]^{2+}$[e]	55	44	22	35
$[Cu(\mathbf{7})]^{+}$[f]	19	26	29	32
$[Cu(CH_3CN)_4]PF_6$[f]	–	40	–	58

[a] NMR yield. [b] Yield after full conversion and after isolation. NMR yield for $[Cu(CH_3CN)_4]PF_6$. [c] Conditions: 40 °C, 42 h. [d] Conditions: 40 °C, 120 h. [e] 10 mol% of catalyst. [f] 20 mol% of catalyst. See Chapter 9 in SI.

$[Cu_2(\mathbf{6})]^{2+}$ and the mono-copper(I) catalyst $[Cu(\mathbf{7})]^{+}$ had turnover numbers close to 1. Importantly, while the above NMR yields may be considered kinetic data, the yields obtained after full conversion and isolation fully agree with $[FeCu_2(\mathbf{1})_2)]^{4+}$ being by far the most efficient catalyst (Table 1).

The time dependence of the click product formation provided further insights. First, we tested the performance of all three copper catalysts in forming the monotriazoles **4a′** and **4b′** (see Scheme 2b and Figure 4: thin lines) but there

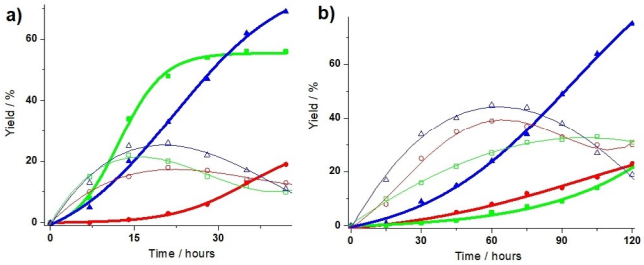

Figure 4. Evolution of products with time from a) **2a**, **DB24C8**, and **3** and from b) **2b**, **DB24C8**, and **3** catalyzed by $[FeCu_2(\mathbf{1})_2]^{4+}$ (blue), $[Cu_2(\mathbf{6})]^{2+}$ (green), or $[Cu(\mathbf{7})]^{+}$ (red). Bold and light lines show yields of "di-click" and "mono-click" products, respectively. For rate constants, see Table S1 in the SI.

was no decisively better yield with any of the catalysts $[FeCu_2(\mathbf{1})_2)]^{4+}$, $[Cu_2(\mathbf{6})]^{2+}$, or $[Cu(\mathbf{7})]^{+}$. The much higher efficiency of $[FeCu_2(\mathbf{1})_2)]^{4+}$ and $[Cu_2(\mathbf{6})]^{2+}$ than that of $[Cu(\mathbf{7})]^{+}$ in producing rotaxane **4a** thus needed explanation. It seems plausible that binding and preorganization of the monotriazole **4a′** at one of the two copper-loaded phenanthrolines increases the effective molarity of the pseudorotaxane at the second catalytic site. The reaction of the longer dialkyne, however, showed a more controversial picture. While formation of monotriazole **4b′** was similar for all catalysts, only catalyst $[FeCu_2(\mathbf{1})_2)]^{4+}$ proved to be highly efficient in the second click reaction; with both $[Cu_2(\mathbf{6})]^{2+}$ and $[Cu(\mathbf{7})]^{+}$ the turnover to **4b** was low.

The possibility of chelate cooperativity suggested to compare the Cu–Cu distances in the double-copper(I) catalysts with the separation of triazole and alkyne units in **4a′** and **4b′** (Figure 5). However, this analysis does not lead to

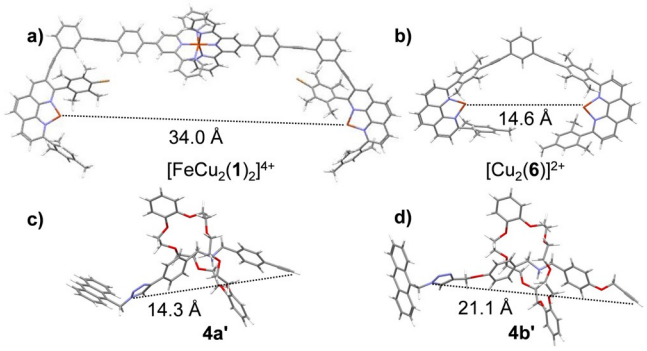

Figure 5. DFT-computed (B3LYP/6-31G(d) + D3(BJ), LANL2DZ for Cu,Fe) distance in a,b) double-copper catalysts and c,d) monotriazoles.

an explanation for all observations. While one would indeed expect the experimental outcome as observed for **2a,b** and $[Cu_2(\mathbf{6})]^{2+}$, that is, a high yield of **4a** due to the perfect distance match of **4a′** and $[Cu_2(\mathbf{6})]^{2+}$ and a low yield of **4b** due to distance mismatch of **4b′** and $[Cu_2(\mathbf{6})]^{2+}$, the pertinent distances in **4a′,b′** and $[FeCu_2(\mathbf{1})_2)]^{4+}$ are not close at all. Nevertheless, the yields of **4a,b** with $[FeCu_2(\mathbf{1})_2)]^{4+}$ are high!

Why are yields high for **4a,b** with $[FeCu_2(\mathbf{1})_2)]^{4+}$ as catalyst despite a clear distance mismatch? A modified hypothesis thus invokes that the monotriazoles **4a′,b′** are bound to both copper centers in the double-copper catalysts if formation of a copper-alkyne η^2-complex is able to compensate for the build-up of strain. As a consequence, we evaluated the thermodynamics of η^2-complex formation within the monotriazole·catalyst complex using DFT-computations (Scheme 3). To model the usual tetra-coordination, the copper(I) center destined for η^2-binding at the terminal acetylene was saturated with two acetonitrile ligands (available from the copper salt). They were liberated in the η^2-binding.

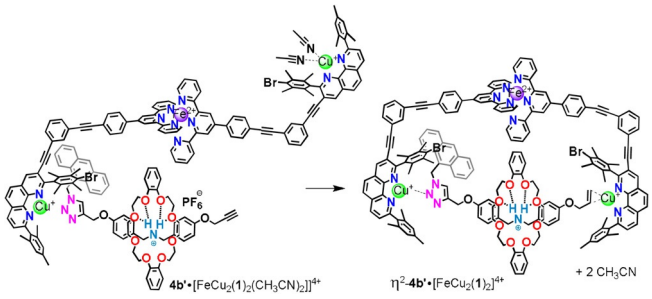

Scheme 3. Reaction for evaluating the thermodynamics of η^2-binding, here illustrated, for example, with **4b′**·$[FeCu_2(\mathbf{1})_2)]^{4+}$. Reaction energies and d_{Cu-Cu} computed by B3LYP/6-31G(d) + D3(BJ), LANL2DZ, including solvent correction.
η^2-binding in **4a′**·$[FeCu_2(\mathbf{1})_2)]^{4+}$: −0.3 kcal mol^{-1} ($d_{Cu-Cu}$ = 16.1 Å)
η^2-binding in **4b′**·$[FeCu_2(\mathbf{1})_2)]^{4+}$: −1.7 kcal mol^{-1} ($d_{Cu-Cu}$ = 20.5 Å)
η^2-binding in **4a′**·$[Cu_2(\mathbf{6})]^{2+}$: −3.3 kcal mol^{-1} (d_{Cu-Cu} = 14.5 Å)
η^2-binding in **4b′**·$[Cu_2(\mathbf{6})]^{2+}$: no minimum found.

The numbers suggest that despite the recognizable deformation of the double-copper catalysts in binding **4a′,b′** at both catalytically active sites (see distances in Figure 5 and Scheme 3), the thermodynamics is favorable in three out of four examples. Incidentally, the favorable thermodynamic cases all show "high-yield" rotaxane formation. It is thus plausible that the increased yield is due to a chelate cooperative effect[10] resulting from the η^2-binding of the intermediate monotriazole which sets up the second click reaction. Notably, the finding that no minimum structure of the triazole/η^2-bound complex **4b′**·$[Cu_2(\mathbf{6})]^{2+}$ was localized is in line with the low yield of **4b** forming in presence of $[Cu_2(\mathbf{6})]^{2+}$, by the way, a yield that is as low as with the mono-copper catalyst $[Cu(\mathbf{7})]^+$. Convincingly, above computed numbers are in good relative agreement with the experimental binding data of **4a′** and **4b′** to $[Cu_2(\mathbf{6})]^{2+}$ (log$K$ = 6.94 and 5.21) and to $[FeCu_2(\mathbf{1})_2)]^{4+}$ (log$K$ = 6.50 and 6.37), see SI, chapter 8. It is important to note that binding in **4b′**·$[Cu_2(\mathbf{6})]^{2+}$ is not stronger than that in **4b′**·$[Cu(\mathbf{7})]^+$ (log$K$ = 5.34). With these data at hand, we readily understand (a) the occurrence of cooperative catalysis in cases with log$K$ > 6, (b) the fast formation of **4a** with $[Cu_2(\mathbf{6})]^{2+}$ (see Figure 4a, green solid line), and (c) the accelerated formation of **4b** with $[FeCu_2(\mathbf{1})_2]^{4+}$ (see Figure 4b, blue solid line).

Presence of a cooperative effect was further supported by probing the efficiency of all catalysts in the mono-click reaction leading to rotaxane **9** (Scheme 4). When a mixture of

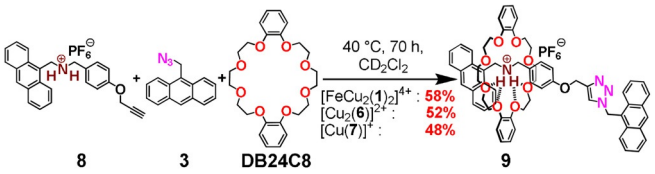

Scheme 4. Synthesis of model rotaxane with all three catalysts.

8, **DB24C8**, and **3** (1:5:4 ratio) was heated at 40 °C for 70 h in presence of 10 mol % of catalyst $[FeCu_2(\mathbf{1})_2)]^{4+}$ or $[Cu_2(\mathbf{6})]^{2+}$ or 20 mol % of $[Cu(\mathbf{7})]^+$, there was no significant difference in the yield of rotaxane **9** (SI, Figures S111, S109 and S107). These results suggest that the cooperative enhancement is only noted in double "click" reactions as solely these profit from the precoordination of the monotriazole intermediate. Incidentally, $[Cu(\mathbf{7})]^+$ chosen as the prototypical click catalyst of this study showed a linear correlation of v_0 (initial rate of catalysis) and the amount of catalyst ruling out the Fokin[18] mechanism (SI, Figure S115).

Finally, from the evolution of yields (Figure 4) it appears that product inhibition may only play a role when there is a perfect match of distances as in the case of $[Cu_2(\mathbf{6})]^{2+}$ and **4a**. In this case we observed the abrupt leveling of the yield at higher conversion (solid green curve in Figure 4a), a feature that was not seen in the other cases. Concerning the formation of **4a** with all catalysts, we were able to experimentally verify (using visual kinetic analysis[19]) that there is no issue of catalyst deactivation and only one case of product inhibition (with catalyst $[Cu_2(\mathbf{6})]^{2+}$, see SI, chapter 9.5) indicating that exact distance matching of triazole and copper sites is not the optimal concept.

Conclusion

We demonstrate here an example of switchable ON/OFF catalysis involving chelate cooperativity.[20] The active catalyst, i.e., complex $[FeCu_2(\mathbf{1})_2]^{4+}$, efficiently catalyzes formation of interlocked rotaxanes via a double-click strategy that was demonstrated to involve complexation of the intermediate monotriazole product at both catalytic sites prior to the second click reaction. A surprising feature of the preorganization is that a close distance match is not the optimal concept. Instead, η^2-complex formation prior to the second click reaction is used to compensate for emerging strain while overcoming the distance differences in catalyst and monotriazole intermediate. As a benefit, once the second triazole is formed, product release is promoted by release of strain in the

$[FeCu_2(\mathbf{1})_2]^{4+}$ catalyst. Due to the importance of the CuAAC strategy[21] for rotaxane formation, the implementation of cooperative and strain effects in double-click strategies should be considered and optimized in future.

Acknowledgements

We are highly indebted to the DFG (Schm 647/19-2 and Schm 647/20-2) and the University of Siegen. Open access funding enabled and organized by Projekt DEAL.

Conflict of Interest

The authors declare no conflict of interest.

Keywords: catalysis · click reaction · cooperativity · rotaxane · supramolecular switch

[1] a) L. van Dijk, M. J. Tilby, R. Szpera, O. A. Smith, H. A. P. Bunce, S. P. Fletcher, *Nat. Rev. Chem.* **2018**, *2*, 117; b) V. Blanco, D. A. Leigh, V. Marcos, *Chem. Soc. Rev.* **2015**, *44*, 5341 – 5370.
[2] a) A. Goswami, M. Schmittel, *Angew. Chem. Int. Ed.* **2020**, *59*, 12362 – 12366; *Angew. Chem.* **2020**, *132*, 12461 – 12465; b) A. Lai, Z. C. Hern, P. L. Diaconescu, *ChemCatChem* **2019**, *11*, 4210 – 4218; c) R. Dorel, B. L. Feringa, *Chem. Commun.* **2019**, *55*, 6477 – 6486; d) S. Gaikwad, A. Goswami, S. De, M. Schmittel, *Angew. Chem. Int. Ed.* **2016**, *55*, 10512 – 10517; *Angew. Chem.* **2016**, *128*, 10668 – 10673.
[3] a) M. Schmittel, P. Howlader, *Chem. Rec.* **2021**, *21*, 523 – 543; b) A. Ghosh, M. Schmittel, *Beilstein J. Org. Chem.* **2020**, *16*, 2831 – 2853.
[4] a) N. Pairault, H. Zhu, D. Jansen, A. Huber, C. G. Daniliuc, S. Grimme, J. Niemeyer, *Angew. Chem. Int. Ed.* **2020**, *59*, 5102 – 5107; *Angew. Chem.* **2020**, *132*, 5140 – 5145; b) H. V. Schröder, C. A. Schalley, *Chem. Sci.* **2019**, *10*, 9626 – 9639; c) J. Y. C. Lim, N. Yuntawattana, P. D. Beer, C. K. Williams, *Angew. Chem. Int. Ed.* **2019**, *58*, 6007 – 6011; *Angew. Chem.* **2019**, *131*, 6068 – 6072; d) C. Biagini, S. D. P. Fielden, D. A. Leigh, F. Schaufelberger, S. Di Stefano, D. Thomas, *Angew. Chem. Int. Ed.* **2019**, *58*, 9876 – 9880; *Angew. Chem.* **2019**, *131*, 9981 – 9985.
[5] a) A. Goswami, S. Gaikwad, M. Schmittel, *Chem. Eur. J.* **2021**, *27*, 2997 – 3001; b) S. De, S. Pramanik, M. Schmittel, *Dalton Trans.* **2014**, *43*, 10977 – 10982.
[6] A. M. Lifschitz, M. S. Rosen, C. M. McGuirk, C. A. Mirkin, *J. Am. Chem. Soc.* **2015**, *137*, 7252 – 7261.
[7] a) L. Benda, B. Doistau, C. Rossi-Gendron, L.-M. Chamoreau, B. Hasenknopf, G. Vives, *Commun. Chem.* **2019**, *2*, 144; b) C. G. Oliveri, P. A. Ulmann, M. J. Wiester, C. A. Mirkin, *Acc. Chem. Res.* **2008**, *41*, 1618 – 1629.
[8] a) M. Raynal, P. Ballester, A. Vidal-Ferran, P. W. N. M. van Leeuwen, *Chem. Soc. Rev.* **2014**, *43*, 1734 – 1787; b) C. G. Oliveri, N. C. Gianneschi, S. T. Nguyen, C. A. Mirkin, C. L. Stern, Z. Wawrzak, M. Pink, *J. Am. Chem. Soc.* **2006**, *128*, 16286 – 16296.
[9] F. Coutrot, *ChemistryOpen* **2015**, *4*, 556 – 576.
[10] L. K. S. von Krbek, C. A. Schalley, P. Thordarson, *Chem. Soc. Rev.* **2017**, *46*, 2622 – 2637.
[11] W. R. Dichtel, J. R. Heath, J. F. Stoddart, *Philos. Trans. R. Soc. A* **2007**, *365*, 1607 – 1625.
[12] a) L. S. Kariyawasam, M. M. Hossain, C. S. Hartley, *Angew. Chem. Int. Ed.* **2021**, *60*, 12648 – 12658; *Angew. Chem.* **2021**, *133*, 12756 – 12766; b) P. Waelès, M. Gauthier, F. Coutrot, *Angew. Chem. Int. Ed.* **2021**, *60*, 16778 – 16799; *Angew. Chem.* **2021**, *133*, 16916 – 16937; c) I. Aprahamian, *ACS Cent. Sci.* **2020**, *6*, 347 – 358.
[13] a) F.-C. Hsueh, C.-Y. Tsai, C.-C. Lai, Y.-H. Liu, S.-M. Peng, S.-H. Chiu, *Angew. Chem. Int. Ed.* **2020**, *59*, 11278 – 11282; *Angew. Chem.* **2020**, *132*, 11374 – 11378; b) T. G. Brevé, M. Filius, C. Araman, M. P. van der Helm, P.-L. Hagedoorn, C. Joo, S. I. van Kasteren, R. Eelkema, *Angew. Chem. Int. Ed.* **2020**, *59*, 9340 – 9344; *Angew. Chem.* **2020**, *132*, 9426 – 9430; c) E. M. Larin, M. Lautens, *Angew. Chem. Int. Ed.* **2019**, *58*, 13438 – 13442; *Angew. Chem.* **2019**, *131*, 13572 – 13576; d) V. K. Tiwari, B. B. Mishra, K. B. Mishra, N. Mishra, A. S. Singh, X. Chen, *Chem. Rev.* **2016**, *116*, 3086 – 3240; e) W. Tanga, M. L. Becker, *Chem. Soc. Rev.* **2014**, *43*, 7013 – 7039.
[14] M. Denis, S. M. Goldup, *Nat. Rev. Chem.* **2017**, *1*, 0061.
[15] I. Paul, A. Ghosh, M. Bolte, M. Schmittel, *ChemistryOpen* **2019**, *8*, 1355 – 1360.
[16] P. Waelès, K. Fournel-Marotte, F. Coutrot, *Chem. Eur. J.* **2017**, *23*, 11529 – 11539.
[17] A. Ghosh, I. Paul, M. Adlung, C. Wickleder, M. Schmittel, *Org. Lett.* **2018**, *20*, 1046 – 1049.
[18] B. T. Worrell, J. A. Malik, V. V. Fokin, *Science* **2013**, *340*, 457 – 460.
[19] C. D.-T. Nielsen, J. Burés, *Chem. Sci.* **2019**, *10*, 348 – 353.
[20] P. Kasinathan, C. Lang, S. Radhakrishnan, J. Schnee, C. D'Haese, E. Breynaert, J. A. Martens, E. M. Gaigneaux, A. M. Jonas, A. E. Fernandes, *Chem. Eur. J.* **2019**, *25*, 6753 – 6762.
[21] M. Meldal, F. Diness, *Trends Chem.* **2020**, *2*, 569 – 584.

Manuscript received: June 22, 2021
Accepted manuscript online: July 21, 2021
Version of record online: August 7, 2021

